

Easy Access to Amides through Aldehydic C–H Bond Functionalization Catalyzed by Heterogeneous Co-Based Catalysts

Cuihua Bai, Xianfang Yao, and Yingwei Li*

School of Chemistry and Chemical Engineering, South China University of Technology, Guangzhou 510640, People's Republic of China

Supporting Information

ABSTRACT: A novel synthesis strategy for amides by oxidative amidation of aldehydes is developed using a heterogeneous Co-based catalyst. The Co composite was prepared by simple pyrolysis of a Co-containing MOF, to obtain well-dispersed Co nanoparticles enclosed by carbonized organic ligands. The catalysts were characterized by powder X-ray diffraction (PXRD), N₂ physical adsorption, atomic absorption spectroscopy (AAS), transmission electron microscopy (TEM), scanning electronic microscopy (SEM), and X-ray photoelectron spectroscopy (XPS). The small Co nanoparticles embedded in the N-doped carbons were highly dispersed with an average size of ca. 7 nm. The Co@C-N materials exhibited significantly enhanced catalytic activity in the oxidative amidation of aldehydes in comparison to those of commercial sources. A series of amides can be easily obtained in good to excellent yields. It was found that the reaction proceeded via radicals under mild conditions, and the carbonyl group in the amide product was from the aldehyde. Moreover, the catalyst could be easily separated by using an external magnetic field and reused several times without significant loss in catalytic efficiency under the investigated conditions.

KEYWORDS: amides, aldehydes, metal–organic frameworks, cobalt, nanoparticles, heterogeneous catalysis



1. INTRODUCTION

Amides are inarguably among the most abundant motifs that are found in biological activities, natural products, pharmaceuticals, and synthetic intermediates.^{1,2} *N,N*-Dimethylformamide (DMF), for example, a widely utilized member of this class of chemicals, is known to be useful as a solvent and also as an important source for O, CO, NMe₂, CONMe₂, Me, and CHO groups in organic reactions.³ The importance of the amides necessitates the development of efficient methodologies for their synthesis.^{2,4–9} The most widely used methods rely on activation of a carboxylic acid and subsequent coupling of the activated species with an amine.^{4,5} More recently, the aminocarbonylation of aryl halides has been developed as a powerful tool for amide preparation.⁶ Other catalytic approaches, such as rearrangement of oximes, carbonylation of alkenes or alkynes, and amidation of nitriles, have also been reported.^{7,8} Despite the considerable achievements that have been made in amide formation, these reaction systems are unfortunately associated with some limitations, such as less readily available starting materials, harsh reaction conditions, and massive production of wastes.⁹ Therefore, the development of a highly efficient and environmentally sound methodology for the synthesis of amides from inexpensive and abundant feedstocks is highly desirable in both academic research and industrial applications.

In view of these findings, oxidative amidation of aldehydes has emerged as an attractive approach for the chemoselective synthesis of amides, due to the economy and formation of environmentally acceptable byproducts.^{9a,b,10–13} In this regard,

Li et al. described a copper-catalyzed procedure that allowed oxidative amidation of aldehydes with amine hydrochloride salts in the presence of silver iodate.¹¹ Wan et al. reported the preparation of amides from oxidation of aldehydes with *N,N*-disubstituted formamides in the presence of TBHP and a catalytic amount of tetrabutylammonium iodide.¹² Wu et al. have developed a Zn(II)-catalyzed oxidative amidation of aldehydes with alkylamines for amides using TBHP as oxidant.¹³ High yields of amides were achieved over these homogeneous systems. Considering the easy separation and reusability of a heterogeneous system, it would be desirable to develop highly efficient heterogeneous catalysts for these transformations.

Herein, we report, for the first time, a cobalt-based catalyst system for the oxidative amidation of aldehydes. Interestingly, the reaction proceeds via acyl radicals under mild conditions to give the corresponding amides in high yields. Moreover, the cobalt-based material can be easily separated from the solution after reaction by using an external magnetic field. Furthermore, the catalyst is reusable and retains high catalytic activity even after recycling for a number of times.

The Co@C-N (carbon–nitrogen embedded cobalt nanoparticle) materials were prepared by simple pyrolysis of a Co(II)-containing metal–organic framework (MOF). MOFs have emerged as a new class of porous materials that are

Received: August 20, 2014

Revised: December 19, 2014

Published: December 23, 2014

assembled with metal ions and organic ligands.¹⁴ Owing to their ordered structures, high surface areas, and large pore volumes, MOFs have been considered as alternative precursors for the preparation of new metal oxides or carbon nanomaterials.¹⁵ These MOF-derived materials have been widely utilized in a variety of fields such as heterogeneous catalysis,¹⁶ electrochemistry,¹⁷ gas adsorption,¹⁸ and sensors.¹⁹ To the best of our knowledge, reports on the use of such MOF-derived materials as catalysts are rare in liquid-phase organic synthesis.

2. EXPERIMENTAL SECTION

2.1. General Information. All chemicals were purchased from commercial sources and used without further purification. ¹H NMR and ¹³C NMR spectra were obtained on a Bruker Avance III 400 spectrometer using CDCl₃ as solvent and tetramethylsilane (TMS) as internal standard. The identification and quantitation of products were performed on a GC-MS spectrometer (Shimadzu GCMS-QP5050A equipped with a 0.25 mm × 30 m DB-WAX capillary column). TGA curves were obtained on a Netzsch STA449C instrument under an argon atmosphere. Powder X-ray diffraction patterns of the samples were obtained on a Rigaku diffractometer (D/MAX-III A, 3 kW) using Cu K α radiation (40 kV, 30 mA, λ = 0.1543 nm). XPS spectra were recorded on Axis Ultra DLD using Mono Al K α (1486.6 eV, 10 mA × 15 kV) as the X-ray source. Atomic absorption spectroscopy (AAS) was obtained on a Hitachi Z-2300 instrument. The size and morphology of the materials were determined by a scanning electronic microscope (SEM, 1530 VP from LEO) equipped with an energy dispersive X-ray detector (EDX, Inca 300 from Oxford) and high-resolution transmission electron microscopy (HR-TEM, C/M300 from Philips). BET surface area and pore size measurements were performed with N₂ adsorption/desorption isotherms at 77 K on a Micromeritics ASAP 2020 M instrument.

2.2. Synthesis of Co^{II}MOF. In a typical synthesis, Co(NO₃)₂·6H₂O (464 mg) was added to a 48 mL 1/1/1 (v/v/v) mixture of *N,N*-dimethylmethanamide (DMF), ethanol, and water containing *tpt* (124 mg) and H₃btc (168 mg) with stirring in a vial. The vial was sealed and heated to 100 °C for 24 h. Red cubic-shaped crystals were formed. The powders were collected by filtration, washed with DMF and ethanol, and then dried in air.

2.3. Synthesis of Co@C-N Materials by Thermolysis of Co^{II}MOF. Typically, 0.5 g of Co^{II}MOF was heated at a high temperature for 8 h with a heating rate of 1 °C/min from room temperature under an argon atmosphere. The as-synthesized material is denoted as Co@C-N x , where x indicates the MOF pyrolysis temperature.

2.4. Procedures for the Oxidative Amidation of Aldehydes with DMF. A mixture of aldehyde (0.5 mmol), TBHP (5 equiv), DMF (2 mL), and catalyst (Co 10 mol %) was placed in a Schlenk tube. The reaction solution was stirred at 80 °C under atmospheric conditions. At the end of the reaction, 100 μ L of *n*-hexadecane as internal standard was added. Then, the catalyst was isolated and a sample of the liquid mixture was subjected to GC-MS analysis. The pure product was obtained by flash column chromatography (1/1 petroleum ether/ethyl acetate).

2.5. Procedures for the Oxidative Amidation of Benzaldehyde with Formamides. A mixture of formamides (2.5 mmol), aldehyde (0.5 mmol), TBHP (5 equiv), toluene (1 mL), and catalyst (Co 10 mol %) was placed in a Schlenk tube.

The tube was sealed, and the mixture was stirred at 100 °C for 24 h. Yields were determined by GC-MS analysis. The pure product was obtained by flash column chromatography (1/1–4/1 petroleum ether/ethyl acetate).

2.6. Recycling of Catalyst. The recyclability of the Co@C-N600 catalyst was investigated for the oxidative amidation of 4-methylbenzaldehyde with DMF under the same reaction conditions as described above, except using the recycled catalyst. Each time, the catalyst was isolated from the solution by magnetic separation after reaction, washed several times with ethanol, dried under vacuum to remove the residual solvent, and then reused as the catalyst in the next run.

3. RESULTS AND DISCUSSION

Co^{II}MOF (Co₉(btc)₆(tpt)₂(H₂O)₁₅; btc = 1,3,5-benzenetricarboxylate, tpt = 2,4,6-tris(4-pyridyl)-1,3,5-triazine) was prepared

Table 1. Surface Areas, Pore Volumes and Sizes, and Chemical Compositions of the Co@C-N Samples

sample	S_{BET} (m ² g ⁻¹)	pore volume (cm ³ g ⁻¹)	pore size (Å)	content (wt %)			
				C ^a	N ^a	H ^a	Co ^b
Co ^{II} MOF	12	0.01	8.9	42.3	7.0	2.3	19.6
Co@C-N500	237	0.08	5.0	64.9	1.8	0.7	30.7
Co@C-N600	251	0.11	4.9	61.0	1.5	0.7	35.8
Co@C-N700	169	0.13	6.2	54.8	1.2	0.6	42.8
Co@C-N800	183	0.18	6.5	53.8	1.0	0.6	44.1
Co@C-N900	179	0.12	6.2	52.9	1.0	0.6	45.3

^aMeasured by elemental analysis. ^bMeasured by AAS.

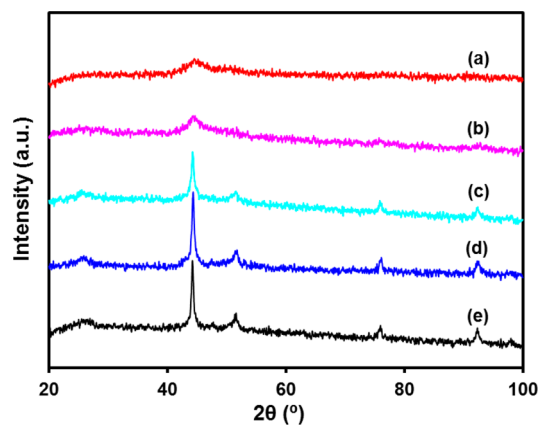


Figure 1. Powder XRD patterns of (a) Co@C-N500, (b) Co@C-N600, (c) Co@C-N700, (d) Co@C-N800, and (e) Co@C-N900.

according to the reported procedures.²⁰ The powder X-ray diffraction (XRD) patterns of the as-synthesized Co^{II}MOF (Figure S1, Supporting Information) were similar to the published XRD data, confirming the formation of pure Co^{II}MOF crystals.²⁰ Co@C-N materials were synthesized by pyrolysis of Co^{II}MOF under a continuous flow of argon. TGA of Co^{II}MOF indicated that the MOF structure began to decompose when the temperature was increased to ca. 400 °C under argon (Figure S2, Supporting Information). Therefore, the calcination temperatures for carbonization of Co^{II}MOF

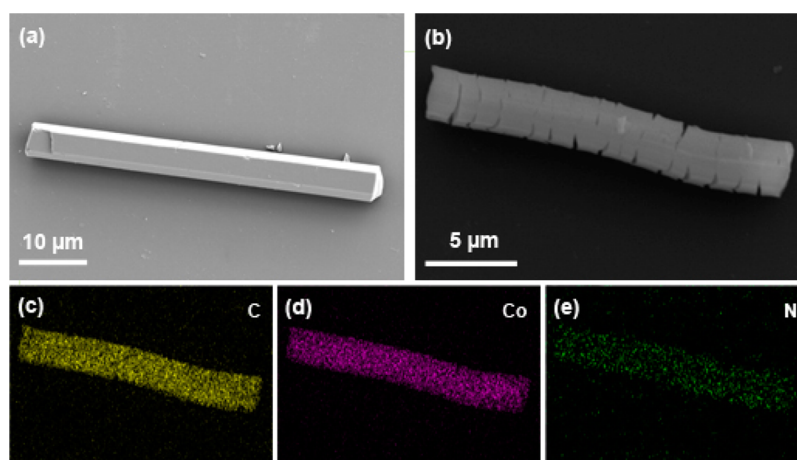


Figure 2. SEM images of (a) the parent Co-MOF, (b) Co@C-N600, and the corresponding (c) C, (d) Co, and (e) N elemental maps.

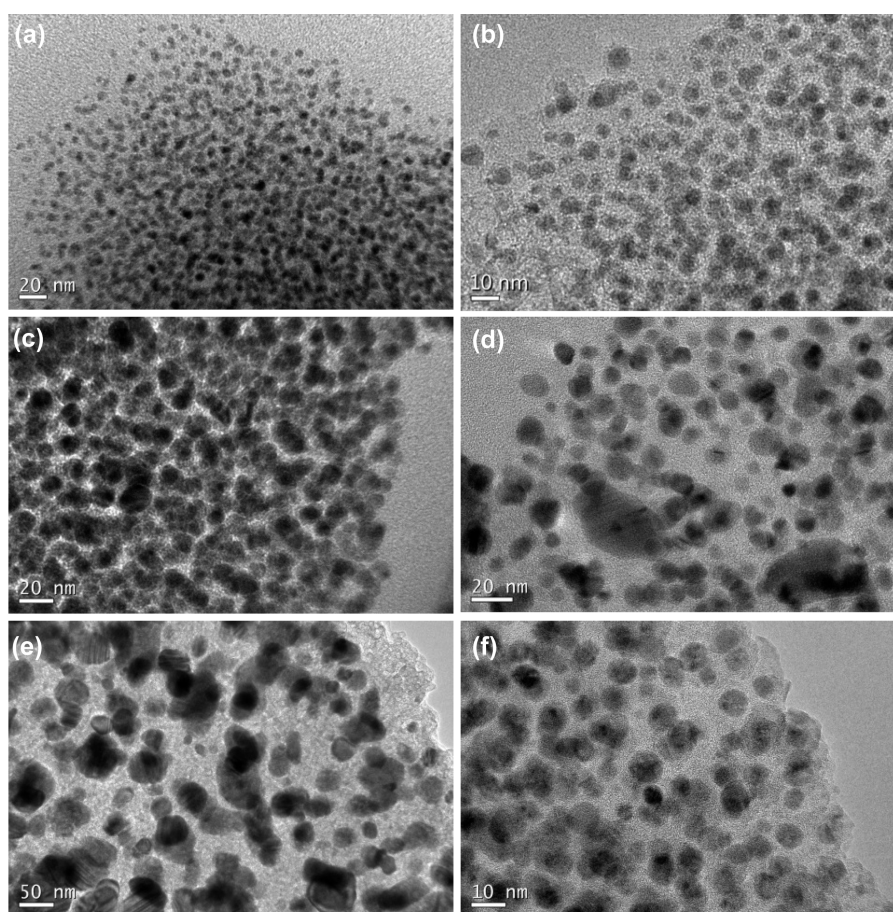
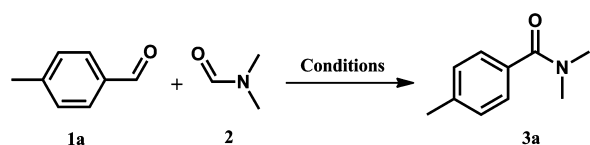


Figure 3. TEM images of (a) Co@C-N500, (b) Co@C-N600, (c) Co@C-N700, (d) Co@C-N800, (e) Co@C-N900, and (f) Co@C-N600 after reaction.

were varied from 500 to 900 °C. The prepared material is denoted as Co@C-N x , where x indicates the MOF thermolysis temperature.

The chemical compositions of the resulting Co@C-N materials were characterized by elemental analysis and AAS. Co, C, N, and H elements were mainly detected, and their weight contents are summarized in Table 1. The quantities of Co in the samples were about 30–45 wt %. The N contents decreased with an increase in the pyrolysis temperature from 500 to 900 °C.

The BET surface areas and porosities of the Co@C-N materials were determined by N₂ adsorption–desorption at 77 K, and the results are shown in Table 1. A very low surface area and pore volume were observed for parent Co^{II}MOF, implying a nonporous structure of the MOF. Notably, the BET surface area and total pore volume showed a remarkable enhancement after decomposition and carbonization of the MOF framework at elevated temperatures, which ranged from 169 to 251 m² g⁻¹ and from 0.08 to 0.18 cm³ g⁻¹, respectively, for the Co@C-N materials.

Table 2. Oxidative Amidation of 4-Methylbenzaldehyde with DMF^a

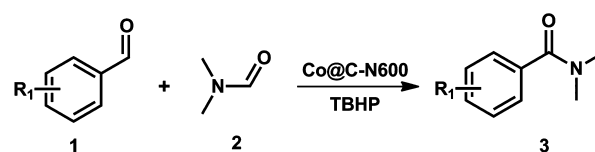
entry	catalyst	oxidant	yield (%) ^b
1	Co@C-N500	TBHP	72
2	Co@C-N600	TBHP	90
3	Co@C-N700	TBHP	56
4	Co@C-N800	TBHP	75
5	Co@C-N900	TBHP	60
6	–	TBHP	3
7	Co(NO ₃) ₂	TBHP	9
8	Co ^{II} MOF	TBHP	32
9	CoO	TBHP	35
10	Co ₃ O ₄	TBHP	34
11	Co	TBHP	14
12	carbon	TBHP	3
13 ^c	Co + carbon	TBHP	18
14	Co@C-N600	–	–
15	Co@C-N600	H ₂ O ₂	–
16	Co@C-N600	O ₂	–
17 ^d	Co@C-N600	TBHP	67

^aReaction conditions (unless specified otherwise): **1a** (0.5 mmol), catalyst (10 mol % Co), oxidant (5 equiv), DMF (2 mL), 80 °C, 24 h. ^bYield was determined by GC-MS analysis. ^c30 wt % Co was mechanically mixed with activated carbon. ^dTBHP (10 equiv).

The XRD patterns of the Co@C-N composites prepared at temperatures below 600 °C showed only one weak and broad peak at ca. 44° (Figure 1). The absence of the diffractions for Co^{II}MOF indicated that the MOF structure was decomposed. Five diffraction peaks at around 44.2, 51.5, 75.8, 92.2, and 97.6° could be observed for the materials calcined at higher temperatures, characteristic of metallic Co (JCPDS No. 15-0806).²¹ The improved intensities of the Co diffraction peaks with an increase in temperature suggested the production of a Co phase with a higher crystallization degree. The XRD diffraction observed at ca. 25° may be assigned to graphite-type carbon sheets (Figure 1c–e).²²

The surface morphology of Co@C-N was determined by SEM (Figure 2), which clearly showed the original shape of Co^{II}MOF crystals. However, the composite surface was distorted with a rough surface, indicating the decomposition and carbonization of the MOF frameworks. Element mapping (Figure 2c–e) revealed a uniform distribution of C, N, and Co in the material. The high dispersion nature of cobalt in the porous N-doped carbons was further demonstrated by high-resolution transmission electron microscopy (HRTEM) (Figure 3). The average size of Co particles in the Co@C-N600 material was around 7 nm (Figure S3, Supporting Information). No significant aggregation of Co nanoparticles was observed, which could be attributed to the isolation effect of carbons formed from carbonization of the tpt and btc linkers in Co^{II}MOF. As the pyrolysis temperature increased, the Co nanoparticles tended to aggregate gradually, as shown in Figure S3.

The catalytic activities of the Co@C-N materials were tested in the oxidative amidation of aldehydes with DMF. First, 4-methylbenzaldehyde (**1a**) was chosen as a model substrate to

Table 3. Scope of the Oxidative Amidation of Various Aldehydes with DMF^e

Entry	Substrate	Product	Time (h)	Yield (%) ^a
1	1a	3a	24	90 (86) ^b
2	1b	3b	24	91
3	1c	3c	24	80
4	1d	3d	24	88
5	1e	3e	20	96
6	1f	3f	16	95
7	1g	3g	36	89
8	1h	3h	36	85
9	1i	3i	36	80
10	1j	3j	36	87
11	1k	3k	36	74
12	1l	3l	36	76
13 ^c	1m	3m	48	50
14 ^c	1n	3n	48	77
15	1o	3o	24	80
16	1p	3p	24	86
17	1q	3q	24	85
18 ^d	1r	3r	24	73

^aYield was determined by GC-MS. ^bIsolated yield. ^c100 °C. ^dReaction conditions: **1r** (0.5 mmol), **2** (2.5 mmol), Co@C-N600 (10 mol % Co), TBHP (5 equiv relative to **1r**), toluene (1 mL), 100 °C. ^eReaction conditions (unless specified otherwise): **1** (0.5 mmol), Co@C-N600 (10 mol % Co), TBHP (5 equiv), DMF (2 mL), 80 °C.

optimize the reaction parameters. A series of solvents, including water, toluene, acetonitrile, and *N,N*-dimethylformamide (DMF), were examined for the reaction. *N,N,N*-4-trimethylbenzamide (**3a**) was obtained in the highest yield in DMF among the investigated solvents (Table S1, Supporting Information). With DMF as the solvent, the prepared Co@C-N materials were all active for the oxidative amidation reaction, and Co@C-N600 exhibited the best catalytic performance to give **3a** in 90% yield at 80 °C (Table 2, entry 2). An increase of temperature to 100 °C led to a remarkable decrease of

Table 4. Scope of the Oxidative Amidation with Various Formamides^a

Entry	Substrate	Product	Yield (%) ^d
1			71
2			76
3			73
4			70
5			68
6			60
7			92
8			87
9			92
10			85
11			61
12			86
13 ^b			77
14 ^c			52

^aYield was determined by GC-MS. ^b36 h. ^cReaction conditions: **1b** (2 mmol), **2n** (0.5 mmol), TBHP (7.5 equiv), 120 °C, 48 h. ^dReaction conditions (unless specified otherwise): **1b** (0.5 mmol), **2b–n** (2.5 mmol), Co@C-N600 (10 mol % Co), TBHP (5 equiv relative to **1**), toluene (1 mL), 100 °C, 24 h.

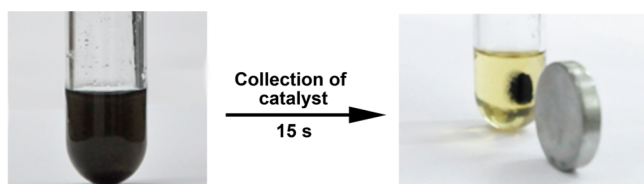


Figure 4. Magnetic separation of the Co@C-N600 catalyst after reaction.

selectivity (Table S1). Blank runs (without a catalyst) gave essentially no activity under identical conditions (Table 2, entry 6).

To verify the unique catalytic characters of the Co@C-N composites, a series of Co-based nanomaterials were also examined in the oxidative amidation reaction for comparison purposes. Homogeneous Co(NO₃)₂ gave a very low catalytic

Table 5. Reusability of Catalyst in the Oxidative Amidation of 4-Methylbenzaldehyde with DMF^a

use	use				
	first	second	third	fourth	fifth
yield (%)	90	88	89	85	87

^aReaction conditions: **1a** (0.5 mmol), Co@C-N600 (10 mol % Co), TBHP (5 equiv), DMF (2 mL), 80 °C, 24 h.

activity (Table 2, entry 7). Similarly, the parent Co^{II}MOF did not show a high activity, and notably, after reaction the MOF structure was observed to be dissolved in the solution (Table 2, entry 8). The use of CoO or Co₃O₄ nanoparticles as catalysts afforded a similarly low yield of **3a** under the investigated conditions (Table 2, entries 9 and 10). In addition, metallic Co nanoparticles (20–30 nm) showed some conversion while activated carbon gave no activity, implying the requirement of a metal to perform the oxidative amidation of aldehydes (Table 2, entries 11 and 12). It was noteworthy that only an 18% yield of **3a** was obtained when using the physical mixture of Co and carbon as catalyst (Table 2, entry 13). These control experiments demonstrated the importance of synergic interactions between the C–N composite and Co nanoparticles in determining the activity of the Co@C–N materials in the oxidative amidation reaction.

Using Co@C-N600 as the catalyst, we further investigated the influence of oxidants on the oxidative amidation of 4-methylbenzaldehyde with DMF. It was observed that, under an inert atmosphere without the addition of an oxidant, no desired product **3a** was obtained (Table 2, entry 14), indicating that oxidant was necessary for the oxidative amidation reaction to proceed. It is worth noting that no amides were detected when other oxidants, such as H₂O₂ and O₂, were employed in the reaction (Table 2, entries 15 and 16). Increasing the amount of oxidant led to a reduced yield due to the formation of *p*-toluic acid as side product (Table 2, entry 17).

With the optimized reaction conditions in hand, we next investigated the oxidative amidation of a wide range of substituted aldehydes with DMF. As shown in Table 3, aromatic aldehydes bearing an electron-donating group in the para, meta, and ortho positions afforded the corresponding substituted *N,N*-dimethyl amides in good to excellent yields within 24 h (entries 1–5). In comparison to the parent molecule (**1b**), the presence of a methyl group in the para and meta positions did not change the yield (entries 1, 2, and 4) remarkably but, when the methyl group was in the ortho position, the yield dropped to 80% due to steric hindrance (entry 3). The higher yield achieved for the substrate **1e** could be attributed to the stronger inductive effect of the methoxy group in the para position (entry 5). 1-Naphthaldehyde also underwent oxidative amidation smoothly and gave **3f** in 95% yield even with less reaction time (Table 3, entry 6). When the reaction time was prolonged to 36 h, phenyl-substituted benzaldehyde was also a compatible substrate for this transformation and furnished the desired amide **3g** in 89% yield (Table 3, entry 7). Under these conditions, 4-fluoro-, 4-chloro-, and 4-bromo-substituted phenyl aldehydes were also selectively amidated at the aldehyde moiety to afford the corresponding amides in 80–87% yields (Table 3, entries 8–10). In general, electron-deficient benzaldehydes exhibited slightly lower activities than electron-rich benzaldehydes (Table 3, entries 11–14). Heteroaryl aldehydes, such as furan-2-carbaldehyde and isonicotinaldehyde, were also amidated with

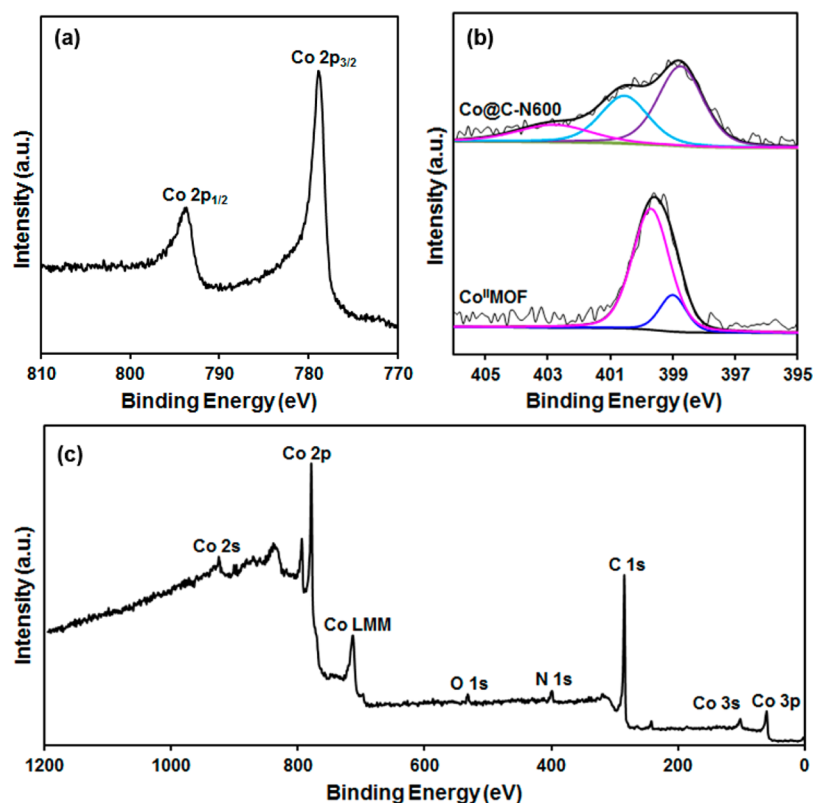


Figure 5. XPS spectra of Co@C-N600 and Co^{II}-MOF: (a) Co 2p of Co@C-N600; (b) N 1s of Co@C-N600 and Co^{II}-MOF; and (c) survey spectrum of Co@C-N600.

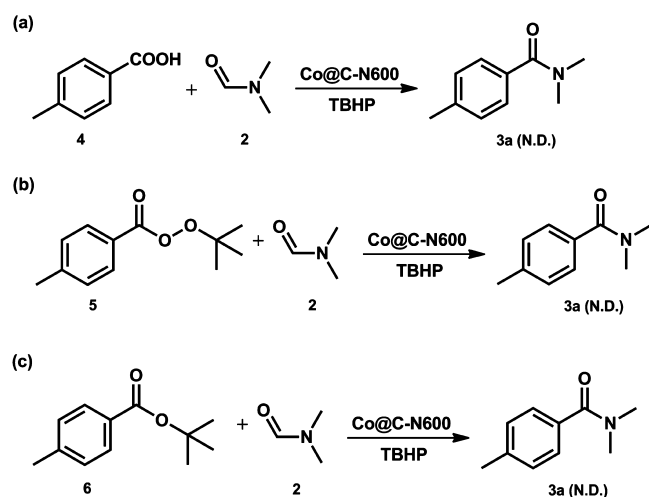


Figure 6. Oxidative amidation of (a) *p*-toluic acid (4), (b) *tert*-butyl perester 5, and (c) *tert*-butyl ester 6 with DMF. N.D.: not detected.

DMF smoothly to provide the desired amides in good yields (Table 3, entries 15 and 16). When aliphatic aldehydes, such as pivalaldehyde, were subjected to the reaction, the corresponding amide products were obtained in good yields using toluene as solvent (Table 3, entries 17 and 18). Notably, the yields of amides shown in Table 3 were comparable to the best results reported in the literature for the oxidative amidation of the same aldehydes with DMF under similar reaction conditions (Table S2, Supporting Information).¹²

The scope of the formamides that can be used in this reaction was studied. First, the reaction parameters were further screened so that the reaction could be applied to various amide

sources (Table S3, Supporting Information). Under the optimized conditions, a range of alkyl-substituted formamides were suitable for the formation of the corresponding amides 8b–g in moderate to high yields (Table 4, entries 1–6). Cyclic and aryl formamides gave 61–92% yields (Table 4, entries 7–12). It was interesting to note that piperazine-1,4-dicarbaldehyde (2n) was selectively amidated with benzaldehyde at one of the formamide groups on the ring to furnish 8n in 77% yield under the optimized conditions (Table 4, entry 13). However, when the reaction time was prolonged and the temperature enhanced with the presence of more benzaldehyde, the double-amidation product 8o was formed in 52% yield (Table 4, entry 14).

The stability and reusability of the Co@C-N600 catalyst were investigated. After the oxidative amidation reaction, the catalyst could be easily separated by placing a magnet near the reactor wall (Figure 4). The recycled catalyst was washed several times with ethanol and then dried under vacuum to remove the residual solvent. As shown in Table 5, the catalyst could be reused at least five times with only a slight loss of activity for the oxidative amidation of 4-methylbenzaldehyde with DMF. The results were in accordance with AAS experiments, in which only traces of Co (less than 0.1% of the total cobalt) were detected in the solution collected by hot filtration after reaction. TEM images (Figure 3f) also showed that no apparent Co aggregation could be observed on the recycled catalyst (Figure S3).

To elucidate the origin of the remarkable activity and stability of the Co@C-N600 catalyst, we further characterized the materials by X-ray photoelectron spectroscopy (XPS). The XPS survey spectrum of Co@C-N600 (Figure 5c) mainly showed the peaks of four elements present in the composite (i.e., C, N,

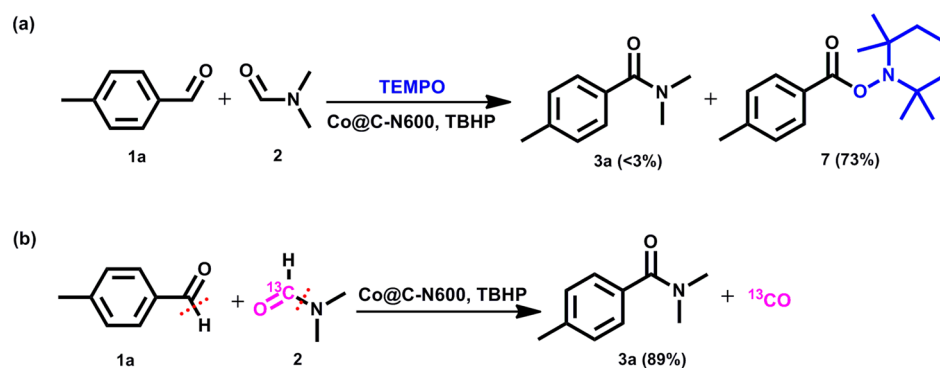


Figure 7. Oxidative amidation of 4-methylbenzaldehyde: (a) with DMF in the presence of 1 equiv of TEMPO and (b) with ^{13}C -labeled DMF.

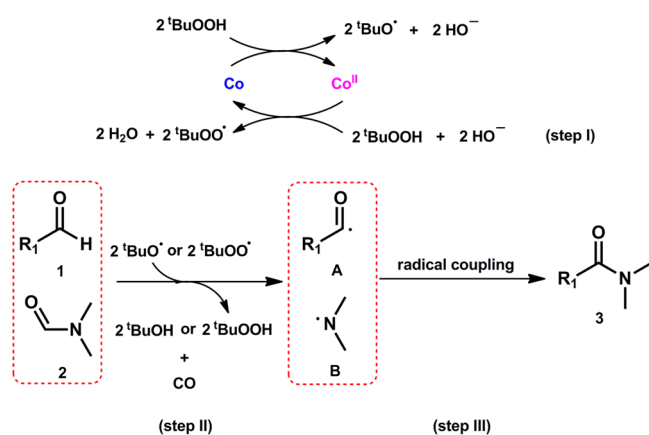


Figure 8. Proposed reaction mechanism for the oxidative amidation of aldehydes with DMF.

O, and Co). Two strong peaks at 793.5 and 778.7 eV, assigned to Co $2p_{1/2}$ and Co $2p_{3/2}$ of metallic Co,²³ respectively, were observed in the XPS spectrum (Figure 5a). The N 1s spectra of Co^{II} MOF showed two binding energies at around 399 and 399.7 eV, which were related to pyridine-type and triazine-type nitrogens, respectively (Figure 5b). However, the N 1s spectra of Co@C-N600 were quite different from those of the pristine Co^{II} MOF material. Three distinct peaks were observed in the N 1s spectra of Co@C-N600 with electron binding energies of 398.8, 400.5, and 402.8 eV, suggesting the presence of three kinds of coordination environments for N atoms. The peak with the lowest binding energy could be attributed to pyridine-type nitrogen that was bonded to a metal.²⁴ Such a coordination interaction between the nitrogen and cobalt was advantageous to prevent a serious aggregation of Co during pyrolysis of the MOF. The N 1s peak at 400.5 eV was assigned to pyrrole-type nitrogen which usually may be found in the carbonized nitrogen-containing organic materials.²⁴ The porous N-doped carbons could exhibit a remarkably enhanced chemical reactivity due to their extended electronic structures.²⁵ The small peak at 402.8 eV was typical for ammonium species.²⁴

To gain more insights into the reaction mechanism of the Co@C-N catalyst system, a series of control experiments were carried out under various conditions. In the oxidative amidation of 4-methylbenzaldehyde with DMF, we observed the formation of a trace amount of *p*-toluic acid (4) in addition to the desired product 3a. In addition, there was a possibility that *tert*-butyl perester 5 or *tert*-butyl ester 6 could also be produced under the reaction conditions (although they were

not detected in the experiments). Thus, we added these three compounds in the reaction instead of an aldehyde (Figure 6). No 3a product was detectable under identical conditions, excluding the involvement of these compounds as intermediates in this transformation. When 1 equiv of TEMPO (2,2,6,6-tetramethylpiperidine-*N*-oxyl, a typical radical inhibitor) was added to the reaction of 4-methylbenzaldehyde with DMF, the TEMPO adduct 7 was predominantly formed instead of the amide 3a in 73% yield (Figure 7a), suggesting that the amidation step might involve a radical pathway. Notably, when DMF was labeled by ^{13}C isotope, the reaction result proved that the carbonyl group in the amide was from the aldehyde, not from the DMF (Figure 7b).

On the basis of the control experiments, it can be concluded that this transformation proceeds via C–H activation of aldehydes involving a radical process.^{9–12} Thus, a possible reaction mechanism is proposed as shown in Figure 8. At the start of the reaction, the *tert*-butoxyl and *tert*-butylperoxyl radicals are generated with the assistance of the cobalt-based catalyst (step I). Then, these radicals abstract hydrogen from the aldehyde and DMF to form acyl radical A and aminyl radical B, respectively (step II). Finally, cross-coupling of the radicals A with B leads to the production of the corresponding amide 3 (step III).

4. CONCLUSIONS

In summary, we have developed a novel, highly efficient, and reusable heterogeneous cobalt-based catalyst for oxidative amidation of aldehydes. The Co@C-N materials are prepared by simple thermolysis of a Co-containing MOF, in which small Co nanoparticles are highly dispersed and enclosed in nitrogen-doped carbons. The materials are highly active in oxidative amidation of a wide range of aldehydes with formamides, affording the corresponding amides in good to excellent yields under mild reaction conditions. A series of control experiments suggest that the reaction proceeds via a novel radical pathway and the carbonyl group in the amide product is from the aldehyde. Moreover, the cobalt-based catalyst is easily recycled and can be reused a number of times without a significant loss of activity. This work would provide an alternative and environmentally benign methodology for the synthesis of amides.

■ ASSOCIATED CONTENT

Supporting Information

The following file is available free of charge on the ACS Publications website at DOI: 10.1021/cs501822r.

Additional characterization and reaction data, spectral data for the products, and ^1H NMR and ^{13}C NMR spectra (PDE)

AUTHOR INFORMATION

Corresponding Author

*E-mail for Y.L.: liyw@scut.edu.cn.

Notes

The authors declare no competing financial interest.

ACKNOWLEDGMENTS

This work was supported by the National Natural Science Foundation of China (21322606 and 21436005), the Doctoral Fund of Ministry of Education of China (20120172110012), the Fundamental Research Funds for the Central Universities (2013ZG0001), and the Guangdong Natural Science Foundation (S2011020002397 and 10351064101000000).

REFERENCES

- (1) (a) Tan, B.; Toda, N.; Barbas, C. F., III *Angew. Chem., Int. Ed.* **2012**, *51*, 12538–12541. (b) Stasi, L. P.; Artusi, R.; Bovino, C.; Buzzi, B.; Canciani, L.; Caselli, G.; Colace, F.; Garofalo, P.; Giambuzzi, S.; Larger, P.; Letari, O.; Mandelli, S.; Perugini, L.; Pucci, S.; Salvi, M.; Toro, P. *Bioorg. Med. Chem. Lett.* **2013**, *23*, 2653–2658. (c) Kuranaga, T.; Sesoko, Y.; Inoue, M. *Nat. Prod. Rep.* **2014**, *31*, 514–532. (d) Kumar, P.; Hornum, M.; Nielsen, L. J.; Enderlin, G.; Andersen, N. K.; Len, C.; Hervé, G.; Sartori, G.; Nielsen, P. *J. Org. Chem.* **2014**, *79*, 2854–2863.
- (2) (a) Allen, C. L.; Williams, J. M. J. *Chem. Soc. Rev.* **2011**, *40*, 3405–3415. (b) Samanta, R.; Matcha, K.; Antonchick, A. P. *Eur. J. Org. Chem.* **2013**, *2013*, 5769–5804. (c) Miyamura, H.; Kobayashi, S. *Acc. Chem. Res.* **2014**, *2014*, 1054–1066.
- (3) (a) Muzart, J. *Tetrahedron* **2009**, *65*, 8313–8323. (b) Ding, S.; Jiao, N. *Angew. Chem., Int. Ed.* **2012**, *51*, 9226–9237. (c) He, T.; Li, H.; Li, P.; Wang, L. *Chem. Commun.* **2011**, *47*, 8946–8948. (d) Niu, Z.; Lin, S.; Dong, Z.; Sun, H.; Liang, F.; Zhang, J. *Org. Biomol. Chem.* **2013**, *11*, 2460–2465. (e) Gao, L.; Tang, H.; Wang, Z. *Chem. Commun.* **2014**, *50*, 4085–4088.
- (4) (a) Al-Zoubi, R. M.; Marion, O.; Hall, D. G. *Angew. Chem., Int. Ed.* **2008**, *47*, 2876–2879. (b) Kumar, P. S.; Kumar, G. S.; Kumar, R. A.; Reddy, N. V.; Reddy, K. R. *Eur. J. Org. Chem.* **2013**, *2013*, 1218–1222. (c) Priyadarshini, S.; Joseph, P. J. A.; Kantam, M. L. *RSC Adv.* **2013**, *3*, 18283–18287. (d) Wang, H.; Guo, L.-N.; Duan, X.-H. *Org. Biomol. Chem.* **2013**, *11*, 4573–4576. (e) Xie, Y.-X.; Song, R.-J.; Yang, X.-H.; Xiang, J.-N.; Li, J.-H. *Eur. J. Org. Chem.* **2013**, *2013*, 5737–5742.
- (5) (a) Gao, J.; Wang, G.-W. *J. Org. Chem.* **2008**, *73*, 2955–2958. (b) Barve, B. D.; Wu, Y.-C.; El-Shazly, M.; Chuang, D.-W.; Chung, Y.-M.; Tsai, Y.-H.; Wu, S.-F.; Korinek, M.; Du, Y.-C.; Hsieh, C.-T.; Wang, J.-J.; Chang, F.-R. *Eur. J. Org. Chem.* **2012**, *2012*, 6760–6766. (c) Mai, W.-P.; Wang, H.-H.; Li, Z.-C.; Yuan, J.-W.; Xiao, Y.-M.; Yang, L.-R.; Mao, P.; Qu, L.-B. *Chem. Commun.* **2012**, *48*, 10117–10119. (d) Jiang, H.; Lin, A.; Zhu, C.; Cheng, Y. *Chem. Commun.* **2013**, *49*, 819–821. (e) Zhao, Q.; Miao, T.; Zhang, X.; Zhou, W.; Wang, L. *Org. Biomol. Chem.* **2013**, *11*, 1867–1873. (f) Barve, B. D.; Wu, Y.-C.; El-Shazly, M.; Chuang, D.-W.; Cheng, Y.-B.; Wang, J.-J.; Chang, F.-R. *J. Org. Chem.* **2014**, *79*, 3206–3214.5.
- (6) (a) Schnyder, A.; Beller, M.; Mehlretter, G.; Nsenda, T.; Studer, M.; Indolese, A. F. *J. Org. Chem.* **2001**, *66*, 4311–4315. (b) Hosoi, K.; Nozaki, K.; Hiyama, T. *Org. Lett.* **2002**, *4*, 2849–2851. (c) Ju, J.; Jeong, M.; Moon, J.; Jung, H. M.; Lee, S. *Org. Lett.* **2007**, *9*, 4615–4618. (d) Jo, Y.; Ju, J.; Choe, J.; Song, K. H.; Lee, S. *J. Org. Chem.* **2009**, *74*, 6358–6361. (e) Sawant, D. N.; Wagh, Y. S.; Bhatte, K. D.; Bhanage, B. M. *J. Org. Chem.* **2011**, *76*, 5489–5494. (f) Sumino, S.; Fusano, A.; Fukuyama, T.; Ryu, I. *Acc. Chem. Res.* **2014**, *47*, 1563–1574.
- (7) (a) Owston, N. A.; Parker, A. J.; Williams, J. M. J. *Org. Lett.* **2007**, *9*, 3599–3601. (b) Fang, X.; Jackstell, R.; Beller, M. *Angew. Chem., Int. Ed.* **2013**, *52*, 14089–14093. (c) Gooßen, L. J.; Arndt, M.; Blanchot, M.; Rudolph, F.; Menges, F.; Niedner-Schatteburg, G. *Adv. Synth. Catal.* **2008**, *350*, 2701–2707.
- (8) (a) Hu, C.; Yan, X.; Zhou, X.; Li, Z. *Org. Biomol. Chem.* **2013**, *11*, 8179–8182. (b) Callens, E.; Burton, A. J.; Barrett, A. G. M. *Tetrahedron Lett.* **2006**, *47*, 8699–8701.
- (9) (a) Reddy, K. R.; Maheswari, C. U.; Venkateshwar, M.; Kantam, M. L. *Eur. J. Org. Chem.* **2008**, *2008*, 3619–3622. (b) Ghosh, S. C.; Ngiam, J. S. Y.; Chai, C. L. L.; Seayad, A. M.; Dang, T. T.; Chen, A. *Adv. Synth. Catal.* **2012**, *354*, 1407–1412. (c) Li, H.; Xie, J.; Xue, Q.; Cheng, Y.; Zhu, C. *Tetrahedron Lett.* **2012**, *53*, 6479–6482. (d) Xu, K.; Hu, Y.; Zhang, S.; Zha, Z.; Wang, Z. *Chem. Eur. J.* **2012**, *18*, 9793–9797.
- (10) (a) Ekoue-Kovi, K.; Wolf, C. *Org. Lett.* **2007**, *9*, 3429–3432. (b) Ekoue-Kovi, K.; Wolf, C. *Chem.—Eur. J.* **2008**, *14*, 6302–6315. (c) Seo, S.; Marks, T. J. *Org. Lett.* **2008**, *10*, 317–319. (d) Li, J.; Xu, F.; Zhang, Y.; Shen, Q. *J. Org. Chem.* **2009**, *74*, 2575–2577. (e) Zhou, B.; Du, J.; Yang, Y.; Li, Y. *Org. Lett.* **2013**, *15*, 2934–2937. (f) Vanjari, R.; Guntreddi, T.; Singh, K. N. *Green Chem.* **2014**, *16*, 351–356.
- (11) Yoo, W.-J.; Li, C.-J. *J. Am. Chem. Soc.* **2006**, *128*, 13064–13065.
- (12) Liu, Z.; Zhang, J.; Chen, S.; Shi, E.; Xu, Y.; Wan, X. *Angew. Chem., Int. Ed.* **2012**, *51*, 3231–3235.
- (13) Zhang, M.; Wu, X.-F. *Tetrahedron Lett.* **2013**, *54*, 1059–1062.
- (14) (a) Perry, J. J., IV; Perman, J. A.; Zaworotko, M. J. *Chem. Soc. Rev.* **2009**, *38*, 1400–1417. (b) Cook, T. R.; Zheng, Y. R.; Stang, P. J. *Chem. Rev.* **2013**, *113*, 734–777. (c) Furukawa, H.; Cordova, K. E.; O’Keeffe, M.; Yaghi, O. M. *Science* **2013**, *341*, 1230444.
- (15) (a) Liu, B.; Shioyama, H.; Akita, T.; Xu, Q. *J. Am. Chem. Soc.* **2008**, *130*, 5390–5391. (b) Chaikittisilp, W.; Ariga, K.; Yamauchi, Y. *J. Mater. Chem. A* **2013**, *1*, 14–19. (c) Lee, H. J.; Cho, W.; Lim, E.; Oh, M. *Chem. Commun.* **2014**, *50*, 5476–5479.
- (16) (a) Zhang, F.; Chen, C.; Xiao, W.-M.; Xu, L.; Zhang, N. *Catal. Commun.* **2012**, *26*, 25–29. (b) Zhao, H.; Song, H.; Xu, L.; Chou, L. *Appl. Catal. A: Gen.* **2013**, *456*, 188–196.
- (17) (a) Yuan, D.; Chen, J.; Tan, S.; Xia, N.; Liu, Y. *Electrochem. Commun.* **2009**, *11*, 1191–1194. (b) Hu, J.; Wang, H.; Gao, Q.; Guo, H. *Carbon* **2010**, *48*, 3599–3606. (c) Liu, B.; Shioyama, H.; Jiang, H.; Zhang, X.; Xu, Q. *Carbon* **2010**, *48*, 456–463.
- (18) (a) Jiang, H.-L.; Liu, B.; Lan, Y.-Q.; Kuratani, K.; Akita, T.; Shioyama, H.; Zong, F.; Xu, Q. *J. Am. Chem. Soc.* **2011**, *133*, 11854–11857. (b) Kim, T. K.; Lee, K. J.; Cheon, J. Y.; Lee, J. H.; Joo, S. H.; Moon, H. R. *J. Am. Chem. Soc.* **2013**, *135*, 8940–8946.
- (19) (a) Hu, M.; Reboul, J.; Furukawa, S.; Torad, N. L.; Ji, Q.; Srinivasu, P.; Ariga, K.; Kitagawa, S.; Yamauchi, Y. *J. Am. Chem. Soc.* **2012**, *134*, 2864–2867. (b) Torad, N. L.; Hu, M.; Kamachi, Y.; Takai, K.; Imura, M.; Naito, M.; Yamauchi, Y. *Chem. Commun.* **2013**, *49*, 2521–2523.
- (20) Chang, Z.; Zhang, D.-S.; Hu, T.-L.; Bu, X.-H. *Cryst. Growth Des.* **2011**, *11*, 2050–2053.
- (21) Nam, K. M.; Shim, J. H.; Ki, H.; Choi, S. I.; Lee, G.; Jang, J. K.; Jo, Y.; Jung, M. H.; Song, H.; Park, J. T. *Angew. Chem., Int. Ed.* **2008**, *47*, 9504–9508.
- (22) Yang, Y.; Jia, L.; Hou, B.; Li, D.; Wang, J.; Sun, Y. *J. Phys. Chem. C* **2014**, *118*, 268–277.
- (23) (a) Biesinger, M. C.; Payne, B. P.; Grosvenor, A. P.; Lau, L. W. M.; Gerson, A. R.; Smart, R. S. C. *Appl. Surf. Sci.* **2011**, *257*, 2717–2730. (b) Wang, D.; Wang, Q.; Wang, T. *Inorg. Chem.* **2011**, *50*, 6482–6492.
- (24) (a) Jagadeesh, R. V.; Junge, H.; Pohl, M. M.; Radnik, J.; Bruckner, A.; Beller, M. *J. Am. Chem. Soc.* **2013**, *135*, 10776–10782. (b) Pels, J. R.; Kapteijn, F.; Moulijn, J. A.; Zhu, Q.; Thomas, K. M. *Carbon* **1995**, *33*, 1641–1653.
- (25) Li, X.-H.; Antonietti, M. *Chem. Soc. Rev.* **2013**, *42*, 6593–6604.